



PERGAMON

Polyhedron 18 (1999) 311–319



POLYHEDRON

# Diethoxy-diphenyl-dithioimidodiphosphinate

Domineco C. Cupertino<sup>a</sup>, Robin W. Keyte<sup>b</sup>, Alexandra M.Z. Slawin<sup>b</sup>,  
J. Derek Woollins<sup>b,\*</sup>

<sup>a</sup> Zeneca Specialties Division, Blackley, Manchester M9 8ZS, UK

<sup>b</sup> Department of Chemistry, Loughborough University, Loughborough, LE11 3TU, UK

Received 16 February 1998; accepted 3 April 1998

## Abstract

Reaction of  $(\text{EtO})_2\text{P}(\text{S})\text{NH}_2$  with  $\text{Ph}_2\text{P}(\text{S})\text{Cl}$  in the presence of NaH gives  $(\text{EtO})_2\text{P}(\text{S})\text{NHP}(\text{S})\text{Ph}_2$  (**1**) which has been complexed with Zn, Pd and Pt in  $\text{Zn}[(\text{EtO})_2\text{P}(\text{S})\text{NP}(\text{S})\text{Ph}_2]_2$  **2**  $\text{Pd}[(\text{EtO})_2\text{P}(\text{S})\text{NP}(\text{S})\text{Ph}_2]_2$  **3**  $\text{Pt}[(\text{EtO})_2\text{P}(\text{S})\text{NP}(\text{S})\text{Ph}_2]_2$  **4** and  $[\text{Pt}(\text{PMe}_3)_2\{(\text{EtO})_2\text{P}(\text{S})\text{NP}(\text{S})\text{Ph}_2\}]^+\text{BPh}_4^-$  **5**. <sup>31</sup>P NMR studies suggest that **3** and **4** are formed as cis/trans mixtures. The X-ray structure of **1** reveals it to be a H-bonded dimer in the solid state, whilst the structures of **3–5** contain  $\text{MS}_2\text{P}_2\text{N}$  rings in varying non-planar (chair, boat) geometries. © 1999 Elsevier Science Ltd. All rights reserved.

**Keywords:** Diethoxy-diphenyl-dithioimidodiphosphinate; Coordination chemistry; Ring conformations

## 1. Introduction

There is considerable interest in the coordination chemistry of  $\text{Ph}_2\text{P}(\text{S})\text{NHP}(\text{S})\text{Ph}_2$  [1–9]. We and others have noted interesting behaviour in the ring conformations of  $\text{MS}_2\text{P}_2\text{N}$  species. Notably less work has been reported on the chemistry of the alkyl analogues  $\text{R}_2\text{P}(\text{S})\text{NHP}(\text{S})\text{R}_2$  with the exception of some studies on  $\text{Me}_2\text{P}(\text{S})\text{NHP}(\text{S})\text{Me}_2$  [10] and  $\text{Pr}_2\text{P}(\text{S})\text{NHP}(\text{S})\text{Pr}_2$  [11]. Some work on unsymmetrical species such as  $\text{Ph}_2\text{P}(\text{O})\text{NHP}(\text{Se})\text{Ph}_2$  has been described [12] and recently there was a report on the synthesis of  $\text{Me}_2\text{P}(\text{S})\text{NHP}(\text{S})\text{Ph}_2$  and its cobalt complex [13]. We have also studied imido-diphosphinates but with varying electronic rather than steric effects, and this latter paper prompts us to report on the synthesis and some coordination chemistry of mixed ethoxy/phenyl substituted dithioimidodiphosphinate. Here we report the synthesis of  $(\text{EtO})_2\text{P}(\text{S})\text{NHP}(\text{S})\text{Ph}_2$  (**1**) together with four examples of its' coordination complexes. The new compounds have

been characterised spectroscopically and in four cases by single crystal X-ray studies.

## 2. Experimental

### 2.1 General

Unless stated otherwise, all reactions were performed under an atmosphere of oxygen-free nitrogen using standard Schlenk procedures. All glassware was oven dried at 100°C or flame dried under vacuum before use.

All solvents and reagents were purchased from Aldrich, BDH or Fisons and used as received. In addition toluene, thf,  $\text{Et}_2\text{O}$  and petroleum ether (60–80) were distilled from sodium-benzophenone under nitrogen, and  $\text{CH}_2\text{Cl}_2$  from  $\text{CaH}_2$ .  $\text{CDCl}_3$  (99+ atom % D) was as supplied.

<sup>31</sup>P (36.2, 101.25, 161.97 MHz) were recorded on JEOL FX90Q, Bruker AC250 or Bruker DPX400 spectrometers. Chemical shifts are reported relative to 85%  $\text{H}_3\text{PO}_4$ . Infra-red spectra were recorded as KBr discs and dichloromethane solutions in Csl cells on a PE System 2000 spectrometer. Raman spectra were recorded on a PE System 2000 with a diode pumped Nd/YAG laser. Microanalyses were carried out by the respective micro-

\* Corresponding author.

analytical services of Loughborough University and Zeneca Specialties Research Centre. FAB +ve mass spectra were recorded by the EPSRC mass spectrometry service at Swansea and the mass spectrometry service at the Zeneca Specialties Research Centre.

## 2.2. Syntheses

$\text{Ph}_2\text{P}(\text{S})\text{Cl}$  was formed by refluxing diphenylchlorophosphine (12.30 g, 10.0 ml, 0.053 mol) with sulfur (1.70 g, 0.053 mol) overnight in toluene (30 ml) under  $\text{N}_2$ . The solvent was evaporated off to give a clear oil (13.31 g;  $^{31}\text{P}$ - $\{^1\text{H}\}$  NMR ( $\text{CDCl}_3$ ):  $\delta$  79.4 ppm).

$\text{Ph}_2\text{P}(\text{S})\text{NH}_2$  was formed by bubbling ammonia gas through a solution of  $\text{Ph}_2\text{P}(\text{S})\text{Cl}$  (4.00 g, 15.84 mmol) in ether (100 ml) for 20 minutes. After filtering the reaction mixture through celite, the filtrate was evaporated to dryness giving a white solid (3.62 g;  $^{31}\text{P}$ - $\{^1\text{H}\}$  NMR ( $\text{CDCl}_3$ ):  $\delta$  59.7 ppm).

$(\text{EtO})_2\text{P}(\text{S})\text{NH}_2$  was formed by bubbling ammonia gas through a solution of diethylchlorothiophosphate (24.00 g, 20.0 ml, 0.127 mol) in ether (100 ml) for 20 minutes. After filtering the reaction mixture through celite, the filtrate was evaporated to dryness to give a clear oil (21.36 g;  $^{31}\text{P}$ - $\{^1\text{H}\}$  NMR ( $\text{CDCl}_3$ ):  $\delta$  74.2 ppm).

### 2.2.1. $(\text{EtO})_2\text{P}(\text{S})\text{NHP}(\text{S})\text{Ph}_2$ **1**

Under anhydrous conditions, sodium hydride (60% dispersion in paraffin oil 1.69 g, 0.042 mol) was slowly added to a solution of  $(\text{EtO})_2\text{P}(\text{S})\text{NH}_2$  (2.38 g, 0.014 mol) in thf (30 ml) at  $0^\circ\text{C}$ . The mixture was allowed to warm to room temperature and stirred for 30 minutes, then  $\text{Ph}_2\text{P}(\text{S})\text{Cl}$  (3.53 g, 0.014 mol) was added dropwise at  $0^\circ\text{C}$ . After addition was complete the mixture was warmed to room temperature and then refluxed overnight. After cooling, methanol (5 ml) was added dropwise to destroy any excess sodium hydride. The volume of the thf was then reduced by half under vacuum and 2M aqueous HCl (50 ml) was added, producing a cloudy white mixture which was washed with dichloromethane ( $3 \times 20$  ml). The dichloromethane was dried over  $\text{MgSO}_4$  then evaporated to dryness to give a white solid **1** which was recrystallised from dichloromethane and hexane (4.22 g, 0.011 mol, 78.3% yield, mp  $62^\circ\text{C}$ ). Microanalysis calculated for  $\text{C}_{16}\text{H}_{21}\text{NO}_2\text{P}_2\text{S}_2$ : C 49.9; H 5.5; N 3.6%. Observed: C 49.8; H 5.4; N 3.6%.  $^{31}\text{P}$ - $\{^1\text{H}\}$  NMR ( $\text{CDCl}_3$ ):  $\delta(\text{P}_1)$  63.6(*d*) [ $\text{P}(\text{OEt})_2$ ],  $\delta(\text{P}_2)$  53.3(*d*) [ $\text{PPh}_2$ ] ppm.  $^2\text{J}$  ( $^{31}\text{P}_\text{A}$ - $^{31}\text{P}_\text{X}$ ) 22.0 Hz. FTIR (dichloromethane solution, CsI plates at 100 microns):  $\nu$  (N–H) 3331  $\text{cm}^{-1}$ ; (KBr disc):  $\nu$  (N–H) 3200,  $\delta$  (N–H) 1298;  $\nu$  (PNP) 976, 768;  $\nu$  (PO) 1190,  $\nu$  (PS) 646, 634  $\text{cm}^{-1}$ .

### 2.2.2. $\text{Zn}[(\text{EtO})_2\text{P}(\text{S})\text{NP}(\text{S})\text{Ph}_2]_2$ **2**

A solution of **1** (0.100 g, 0.260 mmol),  $\text{KO}^t\text{Bu}$  (0.029 g, 0.260 mmol) and  $\text{ZnCl}_2$  (0.018 g, 0.132 mmol) in thf (20 ml) was refluxed for 1 hour. On cooling the mixture was evaporated to dryness and dichloromethane added.

The mixture was then filtered and the filtrate evaporated to dryness yielding a colourless oil. Microanalysis calculated for  $\text{C}_{32}\text{H}_{40}\text{O}_4\text{P}_4\text{S}_4\text{Zn}$ : C 46.1; H 4.8; N 3.4%. Observed: C 49.3; H 6.1; N 3.1%. FTIR (KBr disc):  $\nu$  (PNP) 1239, 764;  $\nu$  (PS) 552, 541;  $\delta$  (NPS) 416  $\text{cm}^{-1}$ . FAB +ve MS:  $m/z$  833 corresponds to  $\{\text{Zn}[(\text{EtO})_2\text{P}(\text{S})\text{NP}(\text{S})\text{Ph}_2]_2\}^+$ .

### 2.2.3. $\text{Pd}[(\text{EtO})_2\text{P}(\text{S})\text{NP}(\text{S})\text{Ph}_2]_2$ **3**

$\text{Pd}(\text{cod})\text{Cl}_2$  (0.050 g, 0.175 mmol) was added to a solution of **1** (0.135 g, 0.351 mmol) and  $\text{KO}^t\text{Bu}$  (0.039 g, 0.348 mmol) in thf (20 ml) and refluxed for 1 hour. The reaction changed colour from yellow to red/orange. On cooling the mixture was evaporated to dryness and dichloromethane added. The mixture was filtered and the filtrate evaporated to dryness. Crystals of **37** were grown from dichloromethane and hexane (0.145 g, 0.166 mmol, 94.7% yield). Microanalysis calculated for  $\text{C}_{32}\text{H}_{40}\text{N}_2\text{O}_4\text{P}_4\text{S}_4\text{Pd}$ : C 43.9; H 4.6; N 3.2%. Observed: C 43.6; H 4.6; N 2.8%. FTIR (KBr disc):  $\nu$  (PNP) 1206, 773;  $\nu$  (PS) 563, 555;  $\nu$  (NPS) 420  $\text{cm}^{-1}$ .

### 2.2.4. $\text{Pt}[(\text{EtO})_2\text{P}(\text{S})\text{NP}(\text{S})\text{Ph}_2]_2$ **4**

$\text{Pt}(\text{cod})\text{Cl}_2$  (0.050 g, 0.134 mmol) was added to a solution of **1** (0.103 g, 0.267 mmol) and  $\text{KO}^t\text{Bu}$  (0.030 g, 0.267 mmol) in thf (20 ml) and refluxed for 1 hour. The reaction changed colour from clear to yellow. On cooling the mixture was evaporated to dryness and dichloromethane added. The mixture was then filtered and the filtrate evaporated to dryness. Crystals of **4** were grown from dichloromethane and hexane (0.118 g, 0.123 mmol, 94.4% yield). Microanalysis calculated for  $\text{C}_{32}\text{H}_{40}\text{N}_2\text{O}_4\text{P}_4\text{S}_4\text{Pt}$ : C 39.9; H 4.2; N 2.9%. Observed: C 41.2; H 3.9; N 3.0%. FTIR (KBr disc):  $\nu$  (PNP) 1255, 1203;  $\nu$  (PS) 576, 542;  $\nu$  (NPS) 426  $\text{cm}^{-1}$ .

### 2.2.5. $[\text{Pt}(\text{PMe}_3)_2\{(\text{EtO})_2\text{P}(\text{S})\text{NP}(\text{S})\text{Ph}_2\}]^+ \text{BPh}_4^-$ **5**

$\text{Pt}(\text{PMe}_3)_2\text{Cl}_2$  (0.060 g, 0.144 mmol) and  $\text{NaBPh}_4$  (0.049 g, 0.143 mmol) were added to a solution of **1** (0.055 g, 0.143 mmol) and  $\text{KO}^t\text{Bu}$  (0.016 g, 0.143 mmol) in thf (30 ml) and refluxed for 1 hour. On cooling the mixture was evaporated to dryness and washed with methanol ( $2 \times 5$  ml). A white solid was filtered off and crystallised from acetone (0.114 g, 0.109 mmol, 75.6% yield). Microanalysis calculated for  $\text{C}_{46}\text{H}_{58}\text{P}_4\text{O}_2\text{S}_2\text{BNPt}$ : C 52.6; H 5.6; N 1.3%. Observed: C 52.2; H 5.6; N 1.1%. FTIR (KBr disc):  $\nu$  (PNP) 1267, 1206, 784;  $\nu$  (PS) 570, 539  $\text{cm}^{-1}$ .

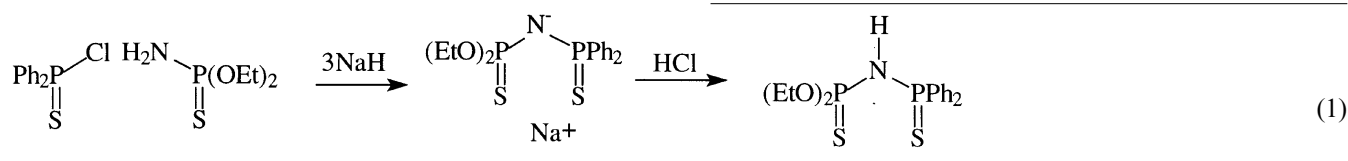
## 2.3. Crystallography

Details of crystallographic parameters are summarised in Table 1. Crystals were mounted on quartz fibres using araldite. Data were collected using  $\text{Cu-K}\alpha$  radiation and  $\omega$  scans at room temperature with a Rigaku AFC7S diffractometer. Intensities were corrected for Lorentz-

polarisation and for absorption. All non-H atoms were refined anisotropically in all cases. The positions of the C–H hydrogen atoms were idealised whilst the N–H atoms were allowed to refine isotropically. Refinements were by full matrix least squares based on  $F$  using teXsan [14]. The weighting scheme is as previously reported [12].

### 3. Results and discussion

The synthesis of **1** was based upon a literature preparation for compounds with mixed substituent groups [15] eq. (1). The amine and halide are ‘clipped’ together with sodium hydride in thf. Excess NaH gave the cleanest products and better yields. Although the reaction may, in principle, be performed using  $\text{Ph}_2(\text{S})\text{NH}_2$  and  $(\text{EtO})_2\text{P}(\text{S})\text{Cl}$  we found that it proceeded in better yield and more cleanly using  $(\text{EtO})_2\text{P}(\text{S})\text{NH}_2$ . The salt was then protonated with dilute hydrochloric acid giving the neutral ligand as an oil which was recrystallised from the minimum of dichloromethane and petroleum ether giving colourless crystals (70–80% yields) pure by elemental analyses. Characteristic bands [10] were observed



in the FTIR,  $\nu(\text{NH})$  ca 3200,  $\delta(\text{NH})$  1298,  $\nu(\text{PO})$  1190,  $\nu(\text{PNP})$  976, 768 and  $\nu(\text{PS})$  646, 634  $\text{cm}^{-1}$  though  $\nu(\text{NH})$  could not be confidently assigned. The  $^{31}\text{P}$  NMR spectrum of **1** ( $\text{CDCl}_3$ , Table 2) is of the AX type. The phosphorus centre with ethoxy substituents appears around 64 ppm as opposed to 53 ppm for the phenyl substituted phosphorus with  $^2\text{J}\{^{31}\text{P}-^{31}\text{P}\}$  coupling of 22.0 Hz in reasonable agreement for disulfur compounds of this type. Solid state  $^{31}\text{P}$  NMR for **1** revealed a doublet as expected (63.5, 52.6 ppm,  $^2\text{J}\{^{31}\text{P}-^{31}\text{P}\} = 22$  Hz) for the two inequivalent phosphorus environments.

By X-ray crystallography **1** exists as a *cisoid* (w.r.t the P=S bonds) dimer in the solid state (Table 3, Fig. a1), the phosphorus with the phenyl substituents being pendant thus reducing any steric crowding. The SP ... PS torsion angle is 87.0° which is comparable to the *cisoid*  $^i\text{Pr}_2\text{P}(\text{S})\text{NHP}(\text{S})\text{P}^i\text{Pr}_2$  [79°] [11]. The P(1)–S(1) bond length at 1.937(1) Å is considerably longer than the pendant P(2)–S(2) bond length of 1.920(2) as a consequence of S(1) being involved in S ... H–N hydrogen-bonding. The P–N bond lengths and the P–N–P bond angle [129.9(2)°] are normal (Fig. 2).

$\text{Zn}[(\text{EtO})_2\text{P}(\text{S})\text{NP}(\text{S})\text{Ph}_2]_2$  (**2**) was obtained by refluxing zinc chloride with two molar equivalents of KO<sup>t</sup>Bu and

**1**. Similarly,  $\text{Pd}[(\text{EtO})_2\text{P}(\text{S})\text{NP}(\text{S})\text{Ph}_2]_2$  (**3**) and  $\text{Pt}[(\text{EtO})_2\text{P}(\text{S})\text{NP}(\text{S})\text{Ph}_2]_2$  (**4**) were obtained from reactions with  $\text{M}(\text{cod})\text{Cl}_2$  as red and yellow solids respectively. In addition one equivalent of **1**, KO<sup>t</sup>Bu and NaBPh<sub>4</sub> were refluxed with  $\text{PtCl}_2(\text{PMe}_3)_2$  in thf to yield  $\text{Pt}(\text{PMe}_3)_2[(\text{EtO})_2\text{P}(\text{S})\text{Ph}_2] + \text{BPh}_4^-$  (**5**, 76% yield). All of the complexes gave reasonable elemental analyses and the FAB +ve mass spectra revealed the expected parent ions. Characteristic bands were observed in the FTIR. High frequency shifts in the  $\nu(\text{PNP})$  vibration from around 950 in the free ligand to 1239–1255  $\text{cm}^{-1}$  are observed upon complexation, whilst the  $\nu(\text{PS})$  vibration shifts from 646 to 552–576  $\text{cm}^{-1}$ —all of these changes reflect the changes in bond order within the ligand due to the delocalisation of the negative charge. The  $^{31}\text{P}$  NMR spectrum (Table 2) of **2** is of the typical AX type. However in **3** and **4** two AX spectra were observed, in each case the chemical shifts were very similar as was the coupling Table 2 and this is most likely due to the presence of the *cis* and *trans* isomers. Alternatively, the crystal structure of **4** suggests (*vide infra*) that there is very little energy difference between the two  $\text{PtS}_2\text{P}_2\text{N}$  ring conformations in the solid state and the two spectra may be due to different ring

conformations in solution. However, calculations [12] suggest the energy difference between ring conformations is too low for this to be a realistic possibility at room temperature. Unfortunately no platinum satellites could be confidently resolved or assigned for any of the spectra. **3** was studied by variable temperature  $^{31}\text{P}$  NMR ( $d^6$ -DMSO). The two AX type spectra observed for **3** were partially resolved in  $d^6$ -DMSO at 298 K whilst at 338 K the signals coalesced (Fig. 3).

The X-Ray structure of **3** reveals (Table 4, Fig. 3) it to be a typical square planar complex with the  $\text{MS}_2\text{P}_2\text{N}$  ring adopting a distorted boat formation. Interestingly the Pd–S(1) bond at 2.325(1) Å is shorter than the Pd–S(2) bond, whereas the S(1)–P(1) bond at 2.207(1) Å is longer than the S(2)–P(2) bond, and the P(1)–N(1) bond is slightly [0.028 Å] longer than the P(2)–N(1) bond of 1.566(3) Å. One could speculate that the electron withdrawing effect of the ethoxy substituents causes the S(2)–P(2) and P(2)–N(1) bonds to be slightly shorter. The Pd–S–P bond angles are 101.09(5) and 110.08(5)° and the S–P–N angles are 116.7(1) and 117.4(1)° whilst the P–N–P angle is 125.1(2)° as expected for a square planar distorted boat type structure [11].

In contrast to **3** in **4** (Fig. 4), one  $\text{MS}_2\text{P}_2\text{N}$  ring adopts

Table 1  
Details of the data collections and refinements for the X-Ray Structures

	(EtO) <sub>2</sub> P(S)NHP(S)Ph <sub>2</sub> (1)	Pd[(EtO) <sub>2</sub> P(S)NP(S)Ph <sub>2</sub> ] <sub>2</sub> (3)	Pt[(EtO) <sub>2</sub> P(S)NP(S)Ph <sub>2</sub> ] <sub>2</sub> (4)	Pt(PMe <sub>3</sub> ) <sub>2</sub> [(EtO) <sub>2</sub> P(S)NP(S)Ph <sub>2</sub> ] <sup>+</sup> BPh <sub>4</sub> <sup>-</sup> (5)
Empirical formula	C <sub>16</sub> H <sub>21</sub> NO <sub>2</sub> P <sub>2</sub> S <sub>2</sub>	C <sub>32</sub> H <sub>40</sub> O <sub>4</sub> P <sub>4</sub> S <sub>4</sub> N <sub>2</sub> Pd	C <sub>32</sub> H <sub>40</sub> O <sub>4</sub> P <sub>4</sub> S <sub>4</sub> N <sub>2</sub> Pt	C <sub>36</sub> H <sub>38</sub> NBO <sub>2</sub> P <sub>4</sub> S <sub>2</sub> Pt
<i>M</i>	385.41	875.21	963.90	1050.88
Crystal colour, habit	clear, block	yellow, needle	yellow, plate	clear, plate
Crystal dimensions/mm	0.21 × 0.21 × 0.32	0.12 × 0.17 × 0.33	0.20 × 0.20 × 0.10	0.15 × 0.05 × 0.50
Space group	P2 <sub>1</sub> /c(#14)	P-1 (#2)	P-1 (#2)	P-1 (#2)
<i>a</i> /Å	13.648(4)	9.710(3)	11.342(6)	14.776(3)
<i>b</i> /Å	9.393(3)	12.554(4)	20.813(5)	17.332(4)
<i>c</i> /Å	15.209(3)	8.890(3)	8.630(6)	9.726(4)
<i>a</i> /°	90	98.95(3)	93.66(3)	102.63(3)
<i>b</i> /°	95.27(2)	91.19(3)	105.44(6)	96.39(3)
<i>g</i> /°	90	112.74(2)	89.51(3)	93.65(2)
<i>U</i> /Å <sup>3</sup>	1941.3(9)	983.3(5)	1959(1)	2405(1)
<i>D<sub>c</sub></i> /gcm <sup>-3</sup>	1.319	1.478	1.633	1.451
<i>μ</i> /mm <sup>-1</sup>	4.1	7.6	10.3	7.9
2θmax/°	120.3	120.2	120.1	119.8
<i>F</i> (000)	808.00	448.00	960.00	1064.00
Independent reflections ( <i>R</i> <sub>int</sub> )	3103 (0.060)	2906 (0.074)	5818 (0.122)	7094 (0.135)
Observed reflections [ <i>I</i> > 3.0σ( <i>I</i> )]	2295	2569	3467	5272
Reflection/parameter ratio	10.98	11.95	8.16	9.89
Minimum/maximum transmission	0.77/1.00	0.77/1.00	0.64/1.00	0.38/1.00
Final <i>R</i> , <i>R</i> '	0.041, 0.039	0.030, 0.041	0.060, 0.059	0.060, 0.068
Maximum <i>D</i> /s	0.20	0.09	2.58	0.08
Largest difference peak hole/eÅ <sup>-3</sup>	0.28	0.40	1.36	1.55

Table 2

Chemical shifts and  $^2J(^{31}\text{P}-^{31}\text{P})$  coupling constants in  $^{31}\text{P}$  NMR ( $\text{CDCl}_3$ ) for  $(\text{EtO})_2\text{P}(\text{S})\text{NHP}(\text{S})\text{Ph}_2$  and  $\text{M}[(\text{EtO})_2\text{P}(\text{S})\text{NHP}(\text{S})\text{Ph}_2]_2$  ( $\text{M}=\text{Zn}, \text{Pd}, \text{Pt}$ ):  $\text{P}_1$  denotes the ethoxy and  $\text{P}_2$  denotes the phenyl substituted phosphorus atoms

	$\delta/\text{ppm}$				$^2J(^{31}\text{P}-^{31}\text{P})/\text{Hz}$	
	$\text{P}_1$			$\text{P}_2$	$[\text{P}_1-\text{P}_2]$	
$(\text{EtO})_2\text{P}(\text{S})\text{NHP}(\text{S})\text{Ph}_2$ 1	63.6			53.3		22.0
$\text{Zn}[(\text{EtO})_2\text{P}(\text{S})\text{NHP}(\text{S})\text{Ph}_2]_2$ 2	46.9			36.3		26.4
$\text{Pd}[(\text{EtO})_2\text{P}(\text{S})\text{NHP}(\text{S})\text{Ph}_2]_2$ 3	50.5	40.5	50.4	40.9	27.5	26.7
$\text{Pt}[(\text{EtO})_2\text{P}(\text{S})\text{NHP}(\text{S})\text{Ph}_2]_2$ 4	44.2	37.8	44.1	38.3	25.6	25.3

Table 3

Selected bond lengths ( $\text{\AA}$ ) and angles ( $^\circ$ ) for  $(\text{EtO})_2\text{P}(\text{S})\text{NHP}(\text{S})\text{Ph}_2$

	1 $(\text{EtO})_2\text{P}(\text{S})\text{NHP}(\text{S})\text{Ph}_2$
S(1)–P(1)	1.937(1)
S(2)–P(2)	1.920(2)
P(1)–N(1)	1.681(3)
P(2)–N(1)	1.667(3)
S(1)–P(1)–N(1)	116.3(1)
S(2)–P(2)–N(1)	112.9(1)
P(1)–N(1)–P(2)	129.9(2)
S–P ... P–S(2)	87.0
N(1)–H(1n)	1.063(2)

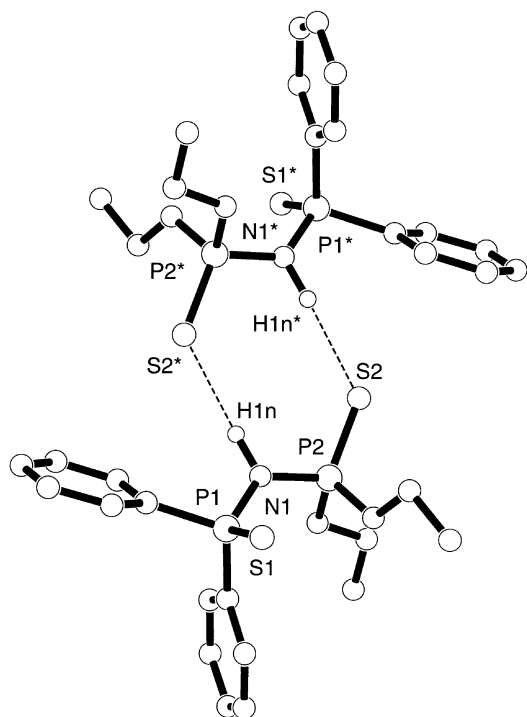


Fig. 1. Crystal structure of  $(\text{EtO})_2\text{P}(\text{S})\text{NHP}(\text{S})\text{Ph}_2$  1 showing the H-bonded dimer.

a distorted boat conformation and the other  $\text{MS}_2\text{P}_2\text{N}$  ring adopts a chair formation, so both known conformations of the  $\text{MS}_2\text{P}_2\text{N}$  ring for are observed in the same compound. Comparing values for the boat and chair conformations in the molecule Table 4, the only significant bond length difference is between the P–N bonds where the P(2)–N(1) length is 0.1  $\text{\AA}$  less than P(1)–N(1) in the boat conformation whereas the P–N bonds are very nearly equal for the chair part of the molecule. The most characteristic difference between the two conformations is in the bond angles. The M–S–P angles for the boat conformation are  $105\text{--}112^\circ$  as opposed to  $100\text{--}102^\circ$  for the chair conformation. The S–P–N angles are all very similar at  $116\text{--}120^\circ$  in contrast to the S–M–S angles which differ quite greatly between all three rings in 3 and 4. The M–S–P angles are slightly smaller for 3 at  $101\text{--}110^\circ$  compared to  $105\text{--}112^\circ$  for 4.

The  $^{31}\text{P}$  NMR of 5 reveals an ABCD type spectrum (Fig. 5, Table 5, the values given in Table 5 were checked using an NMR simulation program) with  $^3J(^{31}\text{P}-^{31}\text{P})$  couplings which was not observed for  $\{\text{Pt}(\text{PMe}_3)_2[\text{N}-(^i\text{Pr}_2\text{PS})_2]\}^+$ .  $\text{P}_A$ ,  $\text{P}_B$  and  $\text{P}_C$  all give well resolved doublets of triplets, though the platinum satellites were partially obscured for  $\text{P}_A$  and  $\text{P}_B$ . *Cis*  $^3J(^{31}\text{P}-^{31}\text{P})$  coupling was found to be of equal magnitude to *trans*  $^3J(^{31}\text{P}-^{31}\text{P})$  coupling for  $\text{P}_A$  and  $\text{P}_B$ . Despite the partial overlap of the triplets in the  $\text{P}_D$  signal seven peaks are observed and the difference between the  $^3J\{^{31}\text{P}_D-^{31}\text{P}_B\}$  *trans* and the  $^3J\{^{31}\text{P}_D-^{31}\text{P}_A\}$  *cis* coupling constants is apparent. It is interesting to note the difference of 8 Hz between the  $^2J(^{31}\text{P}_A-^{195}\text{Pt})$  and  $^2J(^{31}\text{P}_B-^{195}\text{Pt})$  coupling constants as a consequence of the different electronic effects of the substituent groups on  $\text{P}_A$  and  $\text{P}_B$ . This effect could also be explained by the Pt–S–P bond angles (Pt–S– $\text{P}_A$   $108.1^\circ$ , Pt–S– $\text{P}_B$   $97.3^\circ$ ). Given that a larger angle may imply a greater proportion of s character in the hybridised sulfur, this greater proportion of s character is likely to increase the magnitude of the platinum-phosphorus coupling [16].

In the structure of the square planar bis(trimethylphosphine)platinum complex 5 (Fig. 6, Table 6) the  $\text{PtS}_2\text{P}_2\text{N}$  ring shows attributes that have been

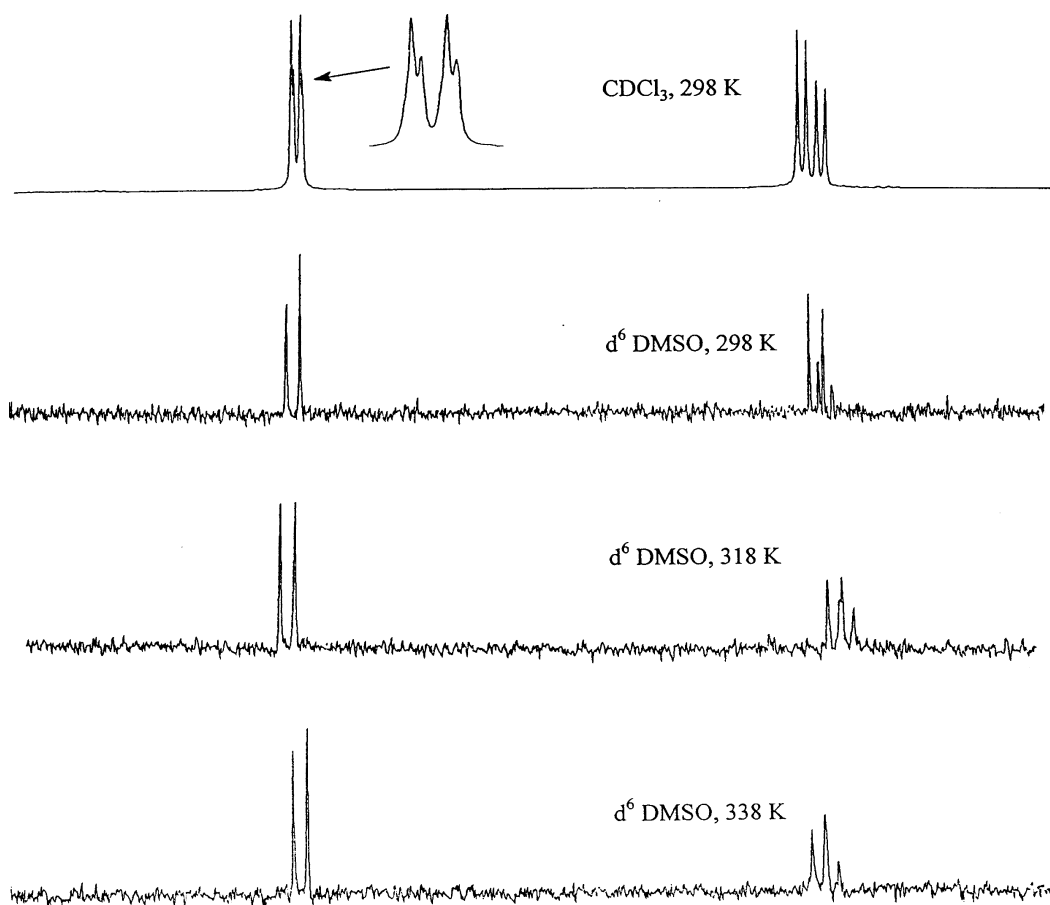


Fig. 2.  $^{31}\text{P}\{-^1\text{H}\}$  VT NMR spectra (36.2 MHz) of  $\text{Pd}[(\text{EtO})_2\text{P}(\text{S})\text{NP}(\text{S})\text{Ph}_2]_2$ .

Table 4  
Selected bond lengths (Å) and angles ( $^\circ$ ) for  $\text{M}[(\text{EtO})_2\text{P}(\text{S})\text{NHP}(\text{S})\text{Ph}_2]_2$  (M = Pd 3, Pt 4)

	3 Boat		4 Chair	
M–S(1)	2.3250(9)	2.338(4)	M–S(3)	2.330(4)
M–S(2)	2.345(1)	2.330(4)	M–S(4)	2.339(4)
S(1)–P(1)	2.027(1)	2.028(6)	S(3)–P(3)	2.207(5)
S(2)–P(2)	2.011(1)	2.008(6)	S(4)–P(4)	2.008(6)
P(1)–N(1)	1.594(3)	1.60(1)	P(3)–N(2)	1.60(1)
P(2)–N(1)	1.566(3)	1.49(2)	P(4)–N(2)	1.57(1)
S(1)–M–S(2)	81.66(3)	100.4(1)	S(3)–M–S(4)	92.8(1)
M–S(1)–P(1)	110.08(5)	105.2(2)	M–S(3)–P(3)	101.8(2)
M–S(2)–P(2)	101.09(5)	111.9(2)	M–S(4)–P(4)	99.5(2)
S(1)–P(1)–N(1)	116.7(1)	116.1(6)	S(3)–P(3)–N(2)	116.4(5)
S(2)–P(2)–N(1)	117.4(1)	118.1(6)	S(4)–P(4)–N(2)	119.9(5)
P(1)–N(1)–P(2)	125.1(2)	127.8(9)	P(3)–N(2)–P(4)	125.1(7)

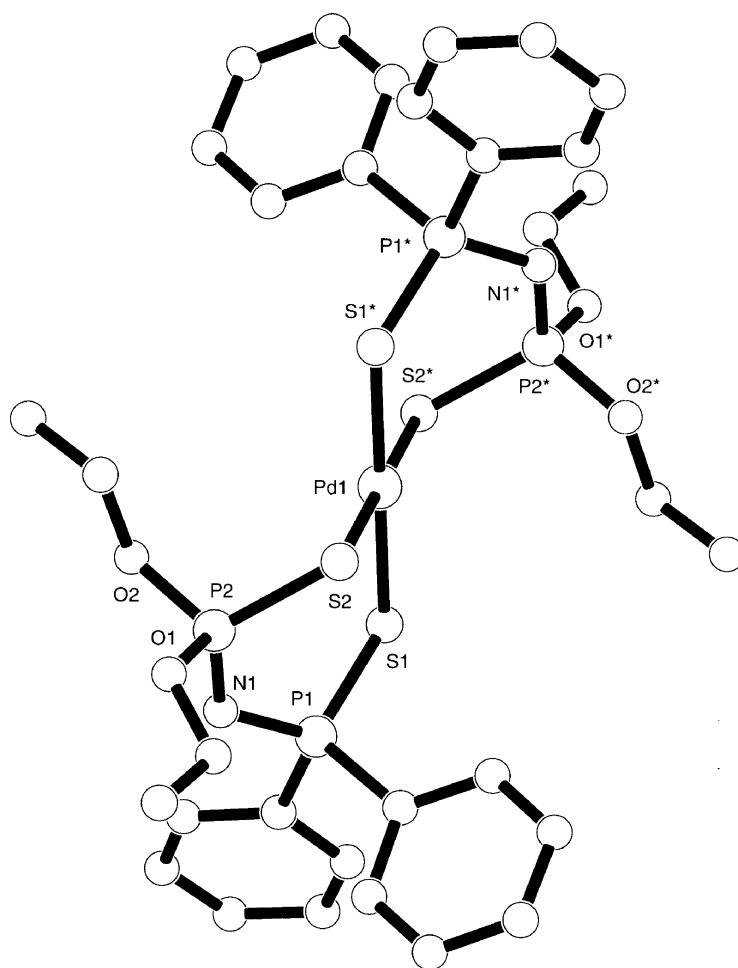
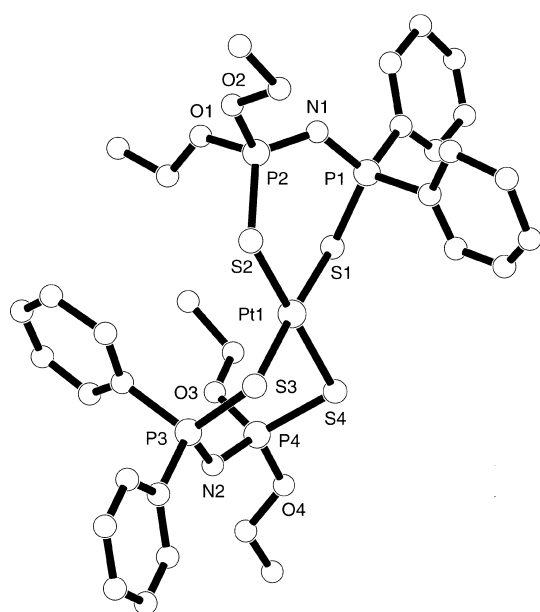
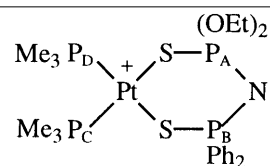
Fig. 3. Crystal structure of Pd[(EtO)<sub>2</sub>P(S)NP(S)Ph<sub>2</sub>]<sub>2</sub> **3**.Fig. 4. Crystal structure of Pt[(EtO)<sub>2</sub>P(S)NP(S)Ph<sub>2</sub>]<sub>2</sub> **4**.

Table 5

<sup>31</sup>P NMR parameters for {Pt(PMe<sub>3</sub>)<sub>2</sub>[(EtO)<sub>2</sub>P(S)NP(S)Ph<sub>2</sub>]}<sup>+</sup>BPh<sub>4</sub><sup>-</sup>

	δ/ppm	[J(P-P)]/Hz				[J(P-Pt)]/Hz Pt
		P <sub>A</sub>	P <sub>B</sub>	P <sub>C</sub>	P <sub>D</sub>	
P <sub>A</sub>	45.9	–	–	–	65.4	–
P <sub>B</sub>	34.3	25.8	–	–	57.5	–
P <sub>C</sub>	–19.8	7.9	9.9	–	–	3104.3
P <sub>D</sub>	–18.0	7.9	9.9	21.8	–	3062.7



observed in square planar ‘chair’, ‘boat’ and tetrahedral complexes. The Pt–S bond lengths differ from each other by 0.02 Å and are 0.03–0.05 Å longer than those in **4**. The difference in Pt–S–P angles is significant, Pt–S(1)–P(1) at 97.3(1)° is consistent with a ‘chair’ type conformation

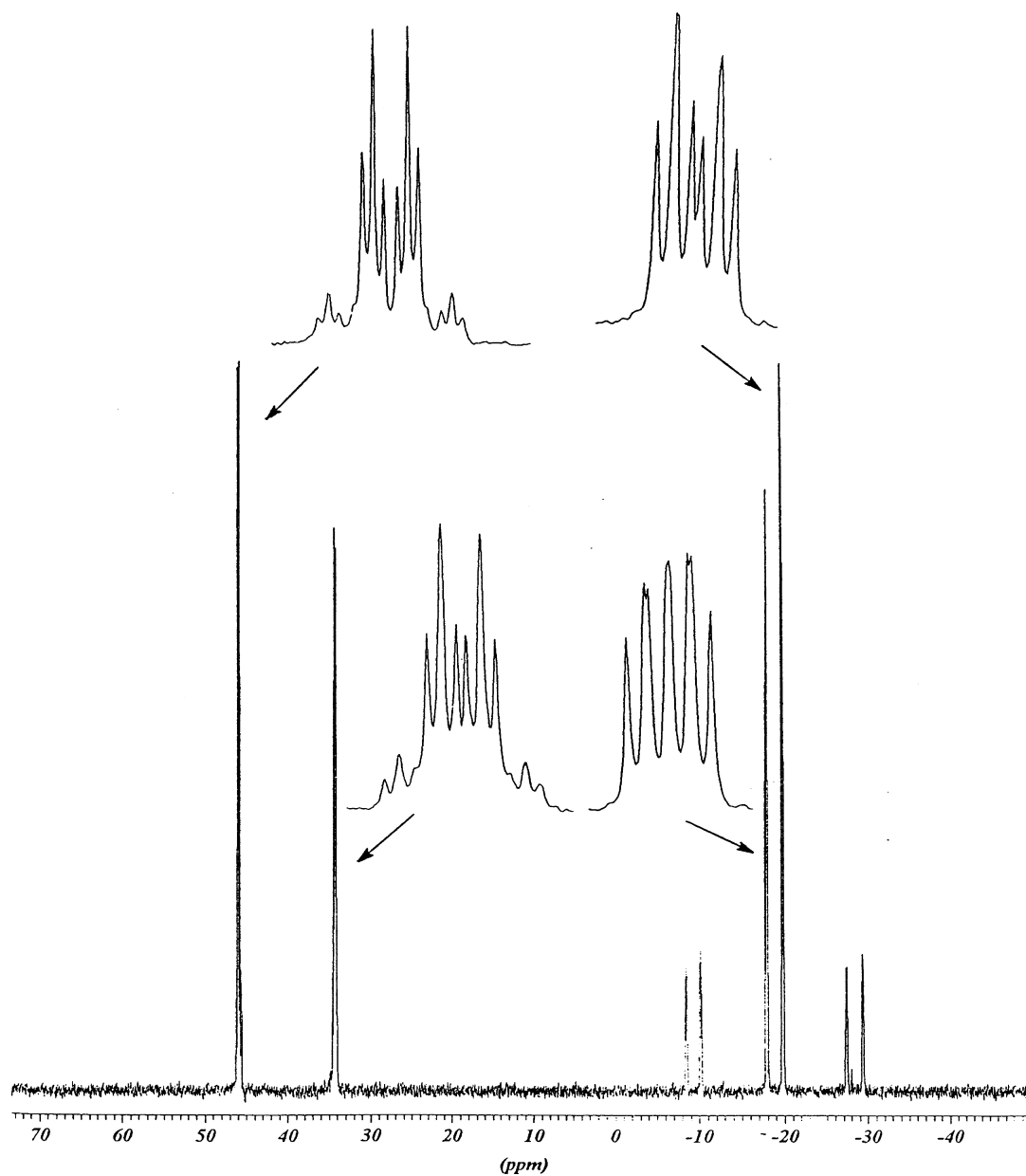


Fig. 5.  $^{31}\text{P}\{-^1\text{H}\}$  NMR spectrum (161.97 MHz) of  $\text{Pt}(\text{PMe}_3)_2[(\text{EtO})_2\text{P}(\text{S})\text{NP}(\text{S})\text{Ph}_2]^+ \text{BPh}_4^-$ .

Table 6  
Selected bond lengths (Å) and angles (°) for  $\{\text{Pt}(\text{PMe}_3)_2[(\text{EtO})_2\text{P}(\text{S})\text{NP}(\text{S})\text{Ph}_2]\}^+\text{BPh}_4^-$  **5**

Bond lengths		Bond angles	
Pt–S(1)	2.371(3)	S(1)–Pt–S(2)	88.7(1)
Pt–S(2)	2.395(3)	Pt–S(1)–P(1)	97.3(1)
Pt–P(3)	2.264(3)	Pt–S(2)–P(2)	108.1(2)
Pt–P(4)	2.276(3)	S(1)–P(1)–N(1)	116.4(4)
S(1)–P(1)	2.026(4)	S(2)–P(2)–N(1)	120.1(4)
S(2)–P(2)	1.987(5)	P(1)–N(1)–P(2)	132.0(6)
P(1)–N(1)	1.608(9)	S(1)–Pt–P(4)	90.9(1)
P(2)–N(1)	1.522(10)	S(2)–Pt–P(3)	86.4(1)
		P(3)–Pt–P(4)	94.6(1)

for the  $\text{PtS}_2\text{P}_2\text{N}$  ring whereas the  $\text{Pt}–\text{S}(2)–\text{P}(2)$  angle of  $108.1(2)^\circ$  implies a ‘boat’ type conformation. Furthermore the large angles of  $\text{S}(2)–\text{P}(2)–\text{N}(1)$  at  $120.1(4)^\circ$  and  $\text{P}(1)–\text{N}(1)–\text{P}(2)$  at  $132.0(6)^\circ$  are more consistent with a tetrahedral ‘boat’ type  $\text{MS}_2\text{P}_2\text{N}$  ring conformation rather than any sort of square planar complex. In this case the  $\text{PtS}_2\text{P}_2\text{N}$  ring can only be described as puckered.

## References

- [1] Woollins JD. *J Chem Soc Dalton Trans* 1996;2893.
- [2] Bhattacharyya P, Novosad J, Phillips J, Williams DJ, Woollins JD. *J Chem Soc Dalton Trans* 1995;1607.
- [3] Bhattacharyya P, Slawin AMZ, Smith MB, Woollins JD. *Inorg Chem* 1996;35:3675.
- [4] Bjernevag S, Husebye S, Maartmann-Moe K. *Acta Chem Scand* 1982;36:195.
- [5] Husebye S, Maartmann-Moe K. *Acta Chem Scand* 1983;37:219.
- [6] Laguna A, Laguna M, Rojo A, Nieves Fraile M. *J Organomet Chem* 1986;315:269.
- [7] Haiduc I, Silvestru C, Roesky H, Schmidt H, Noltemeyer M. *Polyhedron* 1993;12:69.
- [8] Phillips JR, Slawin, AMZ, White AJP, Williams DJ, Woollins, JD. *J Chem Soc Dalton Trans* 1995;2467.
- [9] Bhattacharyya P, Slawin AMZ, Williams DJ, Woollins JD. *J Chem Soc Dalton Trans* 1995;3189.
- [10] Silvestru C, Rosler R, Haiduc I, Cea-Olivares R, Espinosa-Perez G. *Inorg Chem* 1995;34:3352.
- [11] Cupertino DC, Keyte RW, Slawin AMZ, Williams DJ, Woollins JD. *Inorg Chem* 1996;35:2695.
- [12] Slawin AMZ, Smith MB, Woollins JD. *J Chem Soc Dalton Trans* 1996;3659.
- [13] Silvestru C, Rosler R, Drake, JE, Yang J, Espinosa-Perez G, Haiduc I. *J Chem Soc Dalton Trans* 1998;73.
- [14] texSan Crystal Structure Analysis Package, Molecular Structure Corporation, The Woodlands, TX, 1985 and 1992.
- [15] Meznik L, Marecek A. *Z Chem* 1981;8:294.
- [16] Pregosin PS, Kunz RW.  $^{31}\text{P}$  and  $^{13}\text{C}$  NMR of Transition Metal Phosphine Complexes, Diehl P, Fluck E, Kosfeld R, editors. Springer-Verlag, 1979, p. 17.

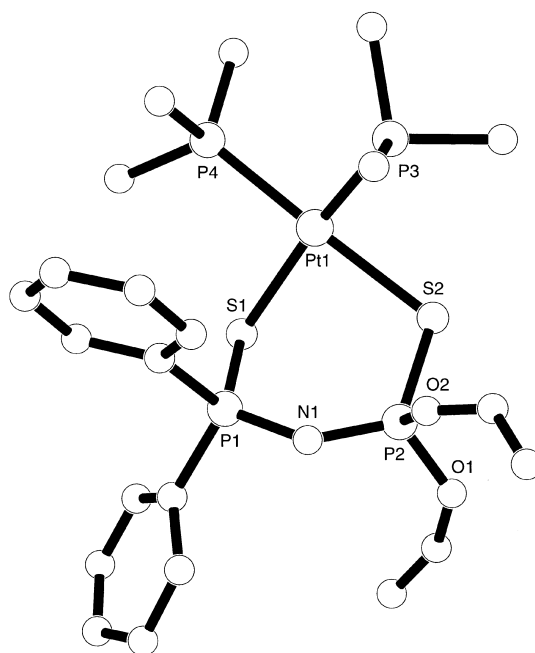


Fig. 6. Crystal structure of  $\{\text{Pt}(\text{PMe}_3)_2[(\text{EtO})_2\text{P}(\text{S})\text{NP}(\text{S})\text{Ph}_2]\}^+$  in **5**.